Evaluation of a multimodal urban arterial: the passenger macroscopic fundamental diagram

Nicolas Chiabaut

CHIABAUT, Nicolas, 2015, Evaluation of a multimodal urban arterial: the passenger macroscopic fundamental diagram, Transportation Research Part B: Methodological, vol 81, Part 2, ELSEVIER, 24 p., DOI: 10.1016/j.trb.2015.02.005

Evaluation of a multimodal urban arterial: the passenger Macroscopic Fundamental Diagram

Nicolas Chiabaut*

* Corresponding author
Email: nicolas.chiabaut@entpe.fr
nicolaschiabaut.weebly.com

Université de Lyon
IFSTTAR / ENTPE
Laboratoire Ingénierie Circulation Transport LICIT
Rue Maurice Audin
F-69518 Vaulx-en-Velin, France

ABSTRACT

This paper aims to extend the concept of Macroscopic Fundamental Diagram (MFD) to combine different transportation modes. Especially, we propose a unified relationship that accounts for cars and buses because the classical MFD is not sufficient to capture the traffic flow interactions of a multimodal traffic. The concept of passenger macroscopic fundamental diagram (p-MFD) is introduced. With this new relationship, the efficiency of the global transport system, i.e. behaviors of cars and buses, can be assessed. Intuitively, the p-MFD shape strongly depends on the mode ratio. Thus, user equilibrium and system optimum are studied and compared. Finally, this relationship is used to design bus system characteristics and to identify the optimal domains of applications for different transit strategies.

1. INTRODUCTION

Cities and transit agencies worldwide have to face an accelerating demand for mobility as people continue to flock to urban areas seeking access to greater economic, educational, and social opportunities. This poses a challenge to optimally distribute city space to multiple transportation modes. To this end, management strategies have to be dynamic, multiscale, and simultaneously applied to individual cars and other transportation modes (such as public transport).

The core element of such management strategies is a global evaluation function of the transportation network. This function must quantify the performance of the whole system that can combine different transportation modes (individual cars, buses, trams, trucks, etc.). This is thus a challenge to capture the traffic dynamics of a complex network mixing these modes. It turns out that cities are complex and intricate systems. Therefore, they are impossible to model in perfect detail. The approach taken in this paper is to look at the transportation network at a macroscopic level. It is important to notice that the approach of the paper is very idealized. Indeed, the challenge here is to propose a modeling framework as general as possible. Then, it could be applied to a relatively wide range of situations and refined based on the characteristics of these situations.

To this end, we resort to an aggregated and parsimonious model to evaluate the transportation network performance. Such a model provides a better understanding and valuable insights on arterial traffic dynamics. The macroscopic fundamental diagram (MFD) can play this role. Indeed, on their seminal works (Godfrey, 1969; Mahmassani et al., 1984; Daganzo, 2007; Geroliminis and Daganzo, 2008), the authors pointed out a major insight: the MFD is an intrinsic property of the network itself and remains invariant when demand changes. The MFD is thus a reliable tool for traffic agencies to manage and evaluate solutions to improve mobility. (Haddad and Geroliminis, 2012; Keyvan-Ekbatani et al., 2012; Aboudoulas and Geroliminis, 2013; De Jong et al., 2013; Chiabaut, 2014; Haddad and Shraiber, 2014; Ramezani et al., 2015) furnished a very good example of how MFDs can be used to model and quantify *ex ante* effects of control. Moreover, recent works (Boyaci and Geroliminis, 2011; Geroliminis and Boyaci, 2012;

Leclercq and Geroliminis, 2013; Xie et al., 2013) propose an accurate method to analytically estimate the MFD for an arterial based on its characteristics (number of lanes, traffic signal parameters, etc.) and the characteristics of the public transport system (Chiabaut et al., 2014).

However, one of the remaining lacks of the MFD is that it only expresses the performance of the system as far as vehicles are concerned. Consequently, the average number of passengers present in each transport mode is not taken into account. Eichler and Daganzo (2006) presented the first instance trying to overcome this drawback. They seek to calculate average the pace for each mode. However, the number of passengers is roughly accounted for and the analysis stays very qualitative according to the authors themselves. Thus we propose in the paper to extend the concept of MFD in order to take into account the number of passengers using the transportation network and not only the number of vehicles. This new relationship is called the passenger Macroscopic Fundamental Diagram (p-MFD). Zheng and Geroliminis (2013), and Chiabaut et al. (2014) have simultaneously introduced the first principles of this relationship.

The mode choice of travelers should be considered as well. It is intuitive that the effect of the ratio of people using public transport rather than individual cars will impact the performance of the transportation network. The p-MFD makes it possible to address this issue and to understand how traffic conditions are modified by the mode choice of passengers. Different equilibriums can be investigated, notably user and system optimums. The ultimate goal of research towards this direction is to develop a strategy that makes people switch from a mode to the other.

The paper is organized as follow: Section 2 introduces the notion of passenger macroscopic fundamental diagram (p-MFD). Section 3 deeply investigates the impacts of modal choice and makes it possible to analytically compare user and system optimums. Section 4 focuses on the application of the p-MFD to network transportation services optimization. Finally, Section 5 proposes a discussion.

2. PASSENGER FUNDAMENTAL DIAGRAM (P-MFD)

In this first section, we extend the definition of MFD to propose a unified relationship that combines all the modes of an urban transportation network: cars, buses, metro, etc. The idea is to relate the number of passengers within the network to space-mean speed of these passengers according to a specific mode choice model. For the sake of simplicity, we first focus on two modes only: individual cars and buses. It is intuitive that, even in this simplest case, the classical MFD is not sufficient to evaluate the performance of the whole network because a bus counts for a unique vehicle. Notice that the methodology presented hereafter is general and can be extended to multiple modes.

2.1. Case study

As mentioned earlier, recent works suggest that there is a consistent relationship between the average network vehicle density and average network flow. Such a relationship is called a MFD. Consequently, we consider in the remainder of the paper an idealized city. Roads shape a very meshed urban network with signalized intersections (see Figure 1a). We also assume that the flows are uniformly distributed among origins and destinations (Leclercq et al., 2014). Under this assumption, car traffic dynamics is well reproduced by a MFD $q(k)$ giving the space-mean flow of cars $q_c=q(k)$ [veh/h] on each link as a function of the space-mean density of the links within the city k [veh/km] (see Figure 1b). Notice that the MFD can now be easily estimated accounting for the effect of buses and control strategies (Geroliminis and Boyaci, 2012; Leclercq and Geroliminis, 2013; Chiabaut et al., 2014). It is also worth noticing that the lower case letters refer to variables expressed in terms of vehicles whereas the upper case letters correspond to variables expressed in terms of passengers. We also assume that the maximal occupancy of a car is ρ_c [pax/veh]. Notice that, for a realistic purpose, we consider that the maximal occupancy is equal to the observed average occupancy (1.2 pax/veh) rather than the effective maximal occupancy (5 pax/veh). We first assume a trapezoidal car MFD for the sake of simplicity. This form is convenient to coarsely mimic the influence of traffic signals. The parameters are the free-flow speed u [km/h], the critical speed u_c, the maximal flow capacity q_x and the jam density k_x. The congested

wave speed is denoted $w=u.q_x/(u.k_x-q_x)$. We assume that all the links are composed of n lanes (n=2).

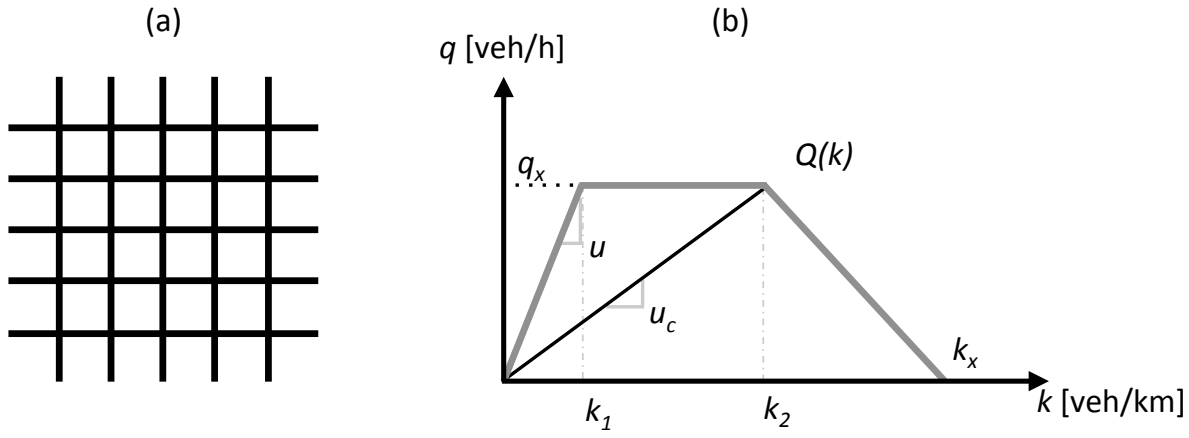

Figure 1: (a) a meshed urban network and (b) its associated car-MFD

We first consider that the public transport system is only composed of buses that share the same roads as the car traffic. We also assume that trips of users can always be realized either by individual car or public transport system. The transit system is characterized by the bus time-headway h [h] and the maximal speed of the buses u_t. We also assume that the maximal occupancy of a bus is ρ_t [pax/bus] and that the buses are mixed with car traffic and no lanes are dedicated to them. Moreover, we consider that the average occupancies of both modes and the number of buses in operation do not depend on the traffic conditions and the mode choice. It turns out that, for a given time-headway h the number of buses n_{bus} in operation is $n_{bus} = L/(h.v_t)$ (Hans et al., 2014) where L [km] is the length of the bus lines of the transportation network and v_t the average speed of the transit system. Physically, it corresponds to static timetables. Finally, Table 1 provides a nomenclature for the different variables and main parameters utilized in the paper. It also provides the values that have been used to draw illustrations.

Variable	Description	Value (if constant)
q	Car MFD [veh/h]	-
q_c	Flow of cars [veh/h]	-
k_c	Density of cars [veh/km]	-
ρ_c	Average occupancy of cars [pax/veh]	1.2
u	Free-flow speed of cars [km/h]	50

u_c	Critical speed of cars [km/h]	7.7
v_c	Average speed of cars [km/h]	-
q_x	Maximal capacity of cars [veh/h]	4250
k_x	Jam density of cars [veh/km]	450
k_1, k_2, k_l	Specific densities of cars [veh/km]	79, 214, 100
w	Congested wave speed [km/h]	18
n	Number of lanes per link [lanes]	3
h	Bus time-headway [h/bus]	-
ρ_t	Maximal occupancies of bus [pax/bus]	40
n_{bus}	Number of bus in operation [bus]	-
L	Length of the transit system [km]	10
v_t	Average speed of the transit system [km/h]	-
u_t	Free-flow speed of the transit system [km/h]	36
P	Total flow of the system [pax/h]	-
F_c	Flow of passengers using cars [pax/h]	-
F_t	Flow of passengers using transit [pax/h]	-
K	Total density of the system [pax/km]	-
K_c	Density of passengers using cars [pax/km]	-
K_t	Density of passengers using transit [pax/km]	-
τ	Mode choice ratio [%]	-
α	Ratio of the network dedicated to transit [%]	-

Table 1: List of main variables and parameters

2.2. The p-MFD

To introduce the p-MFD, the flow is now expressed in terms of passengers per time [pax/h]. Let P denote this flow. P is equal to the sum of passengers using cars F_c and passengers using transit system F_t. It is worth noticing that F_c directly derives from the car MFD $q(k)$ while F_t must be obtained from the characteristics of the transit system. Moreover, as in the classical definition of the MFD, it is thus really appealing to link the flow to the average density of passengers in the city K. However, this is not trivial because K has to be expressed in terms of passengers per space [pax/km]. Moreover, it turns out that the mode choice of passengers between cars and buses has an impact on the flow and density. This ratio is denoted τ and is equal to K_c/K where K_c is the density of passengers using cars.

In this section, τ is considered as static, i.e. constant in time and independent of traffic conditions. Consequently, τ is exogenously given. Physically, it corresponds to an equilibrium situation where day after day the same demand and traffic conditions occur. Notice that these assumptions are relaxed and studied in the forthcoming section. Consequently, the total average flow and the total average density are:

$$\begin{matrix} P(K) = F_c(K_c) + F_t(K_t) \\ K = K_c + K_t \end{matrix} \qquad (1)$$

Where K_c and K_t are respectively the average density in passengers of cars and buses.

It is thus appealing to link P with K and to correctly determine the function $P(K)$ and especially its shape. Consider a given density of passengers K. According to the definition of the mode ratio τ, the density of passenger in cars is $K_c = \tau . K$ [pax/km]. It is worth noticing that this density is also equal to the density of cars weighted by the average occupancy, i.e. $k_c = K_c/\rho_c$ where k_c is the density expressed in [veh/km]. It makes it possible to calculate the average flow in terms of passengers: $F_c = \rho_c . q(k_c) = \rho_c . q(K_c/\rho_c)$ where q is the car MFD. It comes that the associated average speed of passengers using cars is $v_c = q_c/k_c$.

Concerning the transit system, the density of bus passengers is given by $K_t = (1 - \tau).K$ and cannot exceed $\rho_t . n_{bus}/L$ the maximal density of the transit system. Consequently, the associated flow is thus equal to $F_t = \min\left((1-\tau)K, \rho_t n_{bus}/L\right)\Big/_h$. Because we assume that the bus fleet size n_{bus} is constant, i.e. it does depend on traffic conditions, h directly depends on the average speed of the transit system: $h = L/(n_{bus} . v_t)$. Consequently, when the car traffic does not constrain the buses, bus speeds are always equal to the free flow speed u_t and the headway h is not degraded. However, in the case of mixed traffic, congestion may impact the bus system when the speed of the car v_c is lower than the maximal speed of the bus u_t. It comes that $h = L/_{n_{bus}.\min(u_t, v_c)}$ where v_c is the speed of the cars: $v_c = q_c/k_c$.

Finally, equation (1) can be expressed as:

$$P(K) = \rho_c q\left(\frac{\tau K}{\rho_c}\right) + \frac{1}{L}.\min\left((1-\tau)K.L, \rho_t n_{bus}\right).\min(u_t, v_c) \qquad (2)$$

Figure 2 presents the results. The thick gray line corresponds to the car MFD whereas the thin black lines are the different p-MFDs. It is thus appealing to observe the impacts of the bus systems characteristics on the p-MFD shape. To this end, Figure 2a pinpoints the sensitivity of the p-MFD to the bus time-headways *h.* For this application, all the variables are assumed constant except K (and P) and h that ranges between 3 min and 12 min. It turns out that a maximal capacity can be reached for a specific value. Notice that the effect of the bus system on the car traffic dynamics is not accounted here, i.e. the formulation of the car MFD does not depend on the time-headway h. For a given car MFD, it is thus possible to determine the optimal h to maximize the transportation system performance. In the same vein, Figure 2b highlights the impacts of τ on the p-MFD shape. Consequently, the only variables that change are K (and P) and τ that ranges between 0.1 and 1. It is not surprising that the performance can also be optimized for a specific value of τ. It is thus appealing to study in details the impacts of τ and to focus on dynamic τ. This will be investigated in the next section.

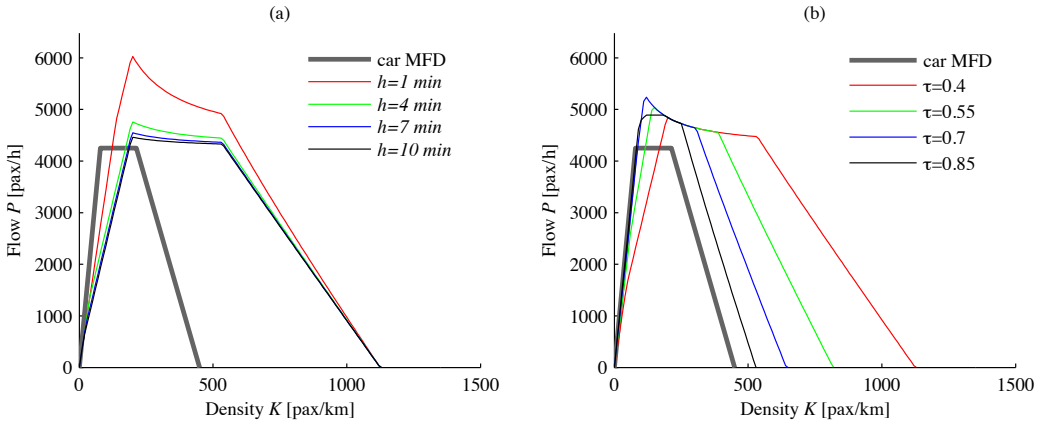

Figure 2: p-MFD for static modal ratio (a) sensitivity to bus time-headway h and (b) sensitivity to mode ratio τ

3. IMPACT OF MODAL CHOICE

Now that we have introduced the concept of p-MFD, this section focuses on the effects of the mode choice and studies the associated equilibrium of the transportation network. Notably, system and user optimums are investigated. To this end, we now consider that the mode choice is based on the utility of the mode. The utility is expressed as the travel cost of using that mode at the beginning of the trip. The travel cost of the whole route

consists of travel time for cars and buses. This very naïve assumption can be refined without changing the general methodology presented hereafter.

3.1. System optimum

We first focus on the system optimum. It corresponds to the second principle of Wardrop. In such an equilibrium situation, the average journey time is minimum, i.e. the average speed of passengers is maximal. It is worth noticing that the speed is equal to the ratio of the demand with the density. Consequently, for a given density K, the associated flow P must satisfy the following equation to maximize the average speed:

$$P(K) = \max_{\tau} \left[\rho_c q \left(\frac{\tau K}{\rho_c} \right) + \frac{1}{L} . \min\left((1-\tau) K . L, \rho_t n_{bus} \right) . \min(u_t, v_c) \right] \quad (3)$$

Based on this equation, we are now able to determine the function P for all the possible traffic conditions, i.e. all the possible values of K.

3.1.1. Free-flow conditions

The free-flow conditions correspond to the situations where the total passenger demand is satisfied by the system. The p-MFD is directly obtained by solving equation (3). Figure 3a presents the resulting p-MFD in case of a trapezoidal car MFD. It turns out that the passenger mode allocation τ is not constant. This is confirmed by Figure 3b that shows the evolution of τ with respect to the passenger density level. Car is the unique mode until the density reaches the critical density k_1 (see Figure 1b), i.e. the demand will exceed the maximal car capacity $\rho_c.q_x$. Then passengers have to switch from cars to the transit system. Note that this corresponds to the optimal situation where passengers are ready to change mode rather than to degrade the traffic conditions. We do not focus in the paper on the possible policies to make users change mode. However, incentive or congestion pricing, traffic information, prescriptive management could be efficient and innovative solutions.

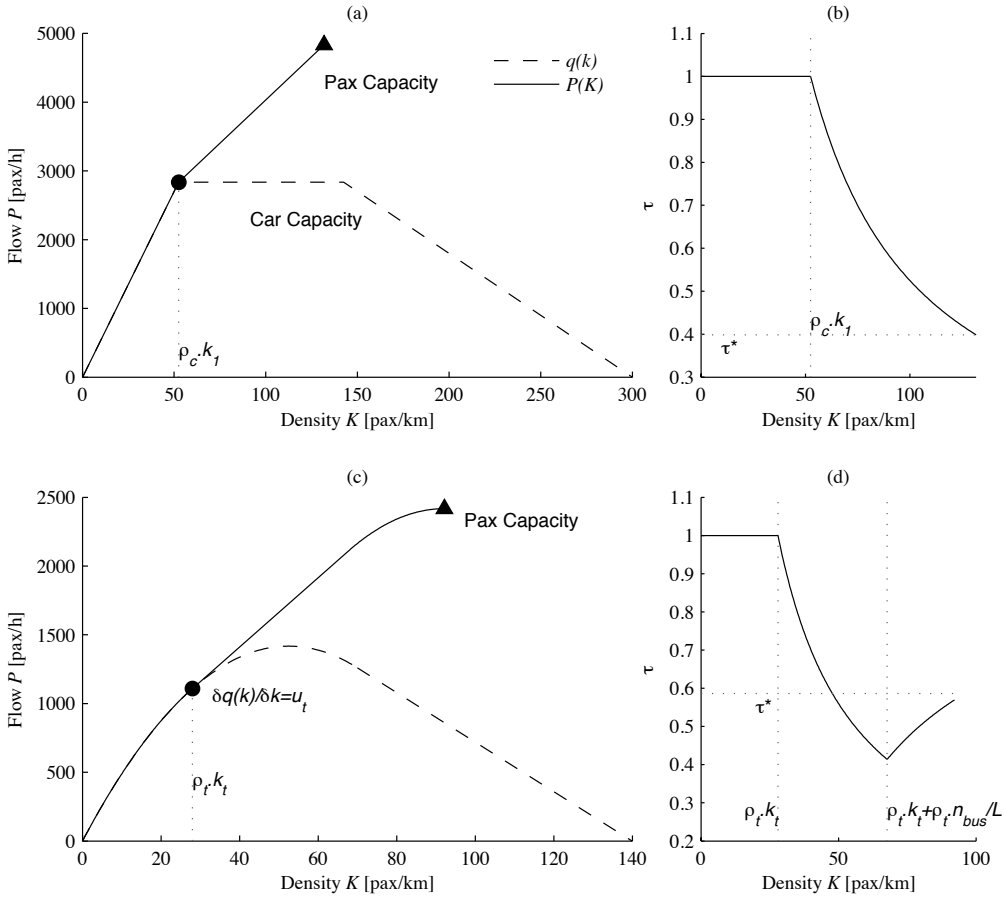

Figure 3: (a) free-flow part of the p-MFD for a trapezoidal MFD and (b) evolution of τ with K (c) free-flow part of the p-MFD for a curved MFD and (d) evolution of τ with K

This method can be applied for any shape of MFD. However, calculations are more complicated. We now assume that the car MFD can take any concave shape. We consider here, for the example, a function composed of a parabolic and linear part (see Figure 3c):

$$Q(k) = ak^2 + bk \text{ for } k < k_l \qquad (4a)$$

$$Q(k) = w(k_x - k_l) \text{ otherwise.} \qquad (4b)$$

Where, $a=-u^2/(2.q_x)$, $b=u$ and $k_l=-(w+b)/(2a)$. Such a formulation ensures to maintain the same free-flow speed than the triangular car MFD.

To determine the associated p-MFD in case of SO, equation (3) has to be re-written as:

$$K(P) = \min_{\tau}(K_c + K_t) \qquad (5)$$

It is also worth noticing that K_c and K_t (respectively) can be expressed as a function of F_c and F_t (respectively). Let us consider F_c^* and F_t^* to be the optimal solution of (5) for a given total density K^*. A small increment ΔF_c and ΔF_t of the flows F_c and Ft will change the density value. This change can be approximated by a first order Taylor expansion:

$$K(F_c^* + \Delta F_c) = K_c(F_c^*) + K_c'(F_c^*).\Delta F_c \qquad (6a)$$

$$K_t(F_t^* + \Delta F_t) = K_t(F_t^*) + K_t'(F_t^*).\Delta F_t \qquad (6b)$$

Thus, the total variation of density is:

$$\Delta K = \Delta P \left(K_c'(F_c^*).\frac{\Delta F_c}{\Delta P} + K_t'(F_t^*).\frac{\Delta F_t}{\Delta P}\right) \qquad (7)$$

This equation can be simplified because if we consider that buses are not affected by traffic congestion, thus: $K_t'(F_t^*) = {}^{1}/_{u_t}$ because $K_t = {}^{n_{bus}.\rho_t}/_{L}$, $F_t = {}^{\rho_t}/_{h}$ and $n_{bus} = {}^{L}/_{h.u_t}$. This is true because we only consider free-flow situations in this section of the paper. It comes:

$$\Delta K = \Delta P \left(\frac{\delta K_c}{\delta F_c}(F_c^*).\frac{\Delta F_c}{\Delta P} + \frac{1}{u_t}.\frac{\Delta F_t}{\Delta P}\right) \qquad (8)$$

ΔK is given by the combination of $\frac{\Delta F_c}{\Delta P}$ and $\frac{\Delta F_t}{\Delta P}$ that minimizes the RHS of equation (8). This quantity admits a lower bound that is equal to $\frac{\delta K_c}{\delta F_c}(F_c^*)$ when $\frac{\delta K_c}{\delta F_c}(F_c^*) < \frac{1}{u_t}$ or to $\frac{1}{u_t}$ otherwise. Thus, it appears that when the total flow varies from ΔP the optimal solution of (8) is only modified for the car flow if $\frac{\delta K_c}{\delta F_c}(F_c^*) < \frac{1}{u_t}$ and for the transit flow otherwise. Consequently, passengers have to shift of mode when $\frac{\delta K_c}{\delta F_c}(F_c^*) = \frac{1}{u_t}$ to reach SO.

Based on these results, the p-MFDs for SO in free-flow conditions are highlighted in Figure 3c. The evolution of τ with respect to the demand level is slightly different from the trapezoidal MFD case, see Figure 3d. To obtain the SO solution, car is the unique mode until a certain car density value that corresponds to k_t such as $\partial q(k_t)/\partial k = u_t$; then passengers switch to the transit system until all the buses are full; finally, the remaining car capacity is used until the system's capacity is reached.

3.1.2. Congested conditions

We now aim to determine the p-MFD when traffic is congested. For cars, the MFD directly accounts for this capacity reduction. For buses, they are not impacted for small congestion, i.e. when $F_c(K_c)/K_c > u_t$. However, when $F_c(K_c)/K_c < u_t$, the buses are slowed down by the queues. Characteristics of the transit system have to be dynamically modified according to $h = {}^{L}/_{n_{bus}.\min(u_t, v_c)}$. It makes it possible to account for congestion in the expression of F_t. Because car-MFD expressed in terms of passengers,

i.e. F_c, also reproduces congested states, the congested part of the p-MFD can be determined according to equation (3). It turns out that equation (3) is only a maximization process that depends on the formulation of F_c and F_t.

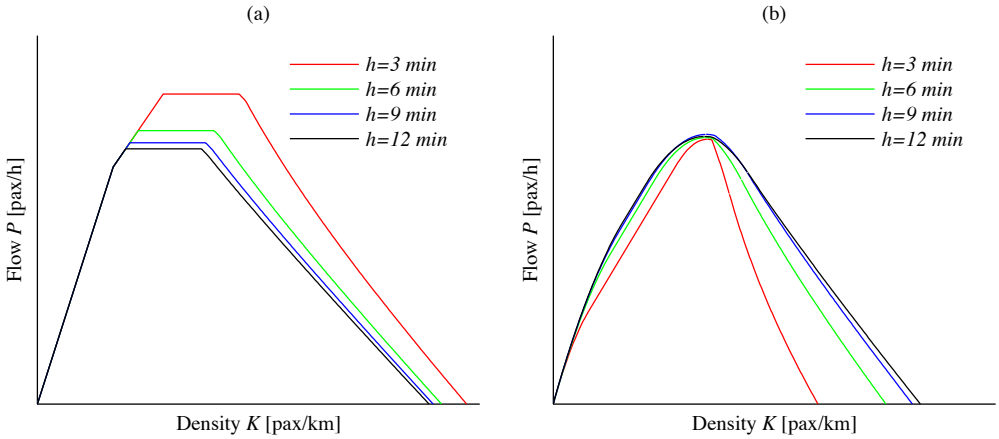

Figure 4: Complete p-MFD in mixed traffic for (a) a car trapezoidal MFD and (b) a car parabolic-linear MFD

Figure 4 presents the associated p-MFD. Figure 4a highlights the influence of the bus time-headways h for a car trapezoidal MFD, i.e. all variables are constant except h that ranges between 3 min and 12 min. It is worth noticing that the transformation is always homothetic because of the linearity of the car MFD shapes. Indeed, for other concave shapes, Figure 4b shows very different results. It is interesting to notice that a specific combination of bus time-headways and car MFDs leads to optimal situations. It is thus appealing to use the p-MFD to determine the optimal bus time-headway for a given situation. It will be studied in Section 4.

3.2. User optimum

We now aim to assess the effect of the mode assignment equilibrium on the associated p-MFD. Indeed, we have only focused on the system optimum since the start of this paper. This assumption is now relaxed to study other modal choice assignment models. Especially, we focus on the Wardrop's first principle and the Logit model.

3.2.1. Wardrop's first principle

The Wardrop's first principle (Wardrop, 1952) can be adapted to our multimodal case. Each user non-cooperatively seeks to minimize his cost of transportation. Consequently, the speeds in all modes actually used equal between them and are higher than those that would be experienced by a single traveller on any unused mode. This principle is referred to as user equilibrium (UE) in the remainder of the paper. Consequently, when the transportation network satisfies the UE, passengers either use only the car or they use both modes.

Figure 5a shows the associated p-MFD in the case of car trapezoidal MFD. It turns out that is still an all-or-nothing situation. Car is the preferred mode until the arterial becomes congested and the speed of the cars becomes the same as the speed of the buses. Then, the passenger demand is split in both modes according to a ratio τ. It is also worth noticing that the difference in terms of flow between the UE and SO is very high (see SO p-MFD in blue). Moreover, these differences occur in free-flow and lead to a capacity reduction in case of UE. It means that the performance of the transportation network can be deeply optimized by managing the demand rather the self-organization situation. Traffic management strategies must focus on free-flow situations that are really close to the system capacity.

Figure 5b highlights the p-MFD for a parabolic-linear car MFD. For this specific shape of car MFD, differences between black and blue lines are smaller but the network performance can still be increased by changing the equilibrium from user to system optimum.

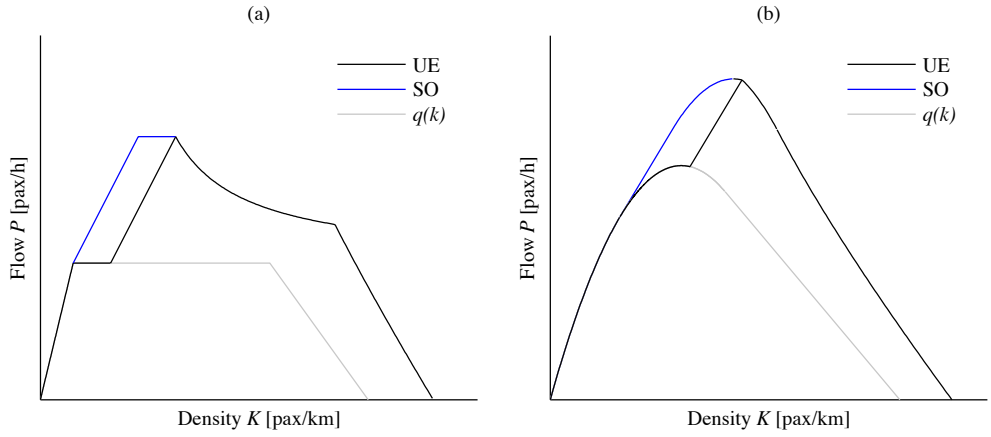

Figure 5: Comparison of UE and SO in case of (a) a car triangular MFD (b) a parabolic-linear MFD

3.2.1. The Logit model

In the vein of Leclercq and Geroliminis (2013), the Logit model can also be easily adapted to a multimodal traffic. The associated situation is referred to as stochastic user equilibrium (SUE) in the remainder of the paper. We now assume that the ratio of flows between cars and buses only depends on the difference in travel times, i.e. speed, between both modes:

$$\frac{F_t}{F_c} = e^{-\theta\left(\frac{L}{v_t}-\frac{L}{v_c}\right)} \qquad (9)$$

Where θ is the parameter of the Logit model and L the average trip length.

We have now all the equations to formulate a parametric expression of the flow P for the arterial with respect to v_c. This defines a simple method to calculate the p-MFD for the Logit model. Figure 6 presents the resulting p-MFD. Notice that all the variables are constant except θ. Therefore, we have tested several θ values (from 0.05 to 0.9 with an increment of 0.05). It turns out that p-MFDs fall between UE and SO. Moreover, UE, SUE and SO only differ at the network level in free-flow situations when average speed is comprised between u and u_t for trapezoidal MFD and u_s and u_t for curved MFD (u_s such as $\frac{\delta F_c}{\delta K_c} = u_t$). This is not surprising because in congestion both modes have the same speed. The mode ratio is then constant.

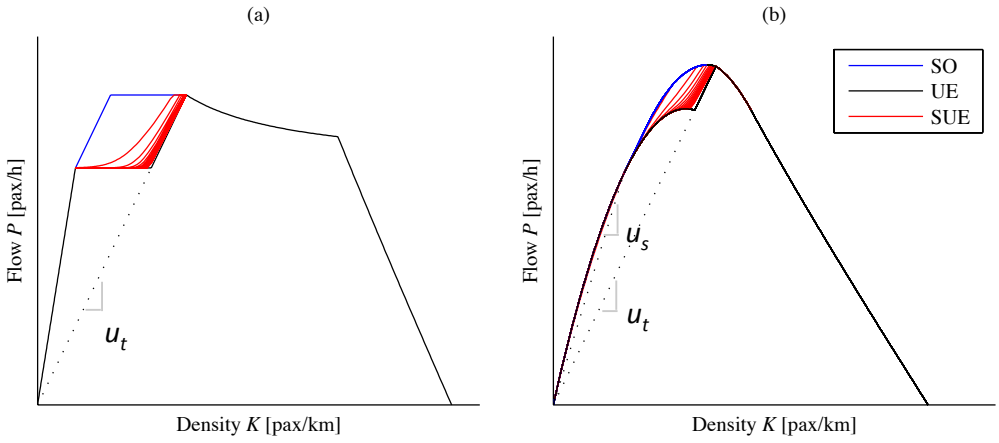

Figure 6: Comparison of SUE, UE and SO in case of (a) a car trapezoidal MFD (b) a parabolic-linear MFD

3.2.2. Equilibriums comparison

Even if rough comparisons between UE and SO are proposed by Figure 5a, it is still appealing to study these difference in more detail. To this end, we now focus on the marginal costs of UE and SO. This will give useful insights on the pricing policy that can be implemented to adapt the costs of each mode and switch the transportation network from UE to SO.

The marginal cost of a mode defines the increase of the cost of this mode if one more passenger chooses to use this mode. The marginal cost of mode i is obtained by differentiating the cost function $c_i(K_i)$:

$$MC_i(K_i) = c_i(K_i) + K_i c_i'(K_i) \qquad (10)$$

Here the cost of a mode is characterized by the average speed, i.e. $c_i = F_i(K_i)/K_i$. Thus, the derivative c_i' can be formulated as:

$$c_i'(K_i) = \frac{K_i F'(K_i) - F(K_i)}{K_i^2} \qquad (11)$$

Finally, the marginal costs of each mode are equal to:

$$\begin{aligned} MC_c(K_c) &= F_c'(K_c) = \frac{\delta F_c(K_c)}{\delta K_c} \\ MC_t(K_t) &= F_t'(K_t) = \frac{\delta F_t(K_t)}{\delta K_t} \end{aligned} \qquad (12)$$

With this pricing, SO is reached by letting the system self-organized, i.e. Wardrop's user equilibrium. The conditions of SO highlighted in the previous section can be identified. It turns out that the demand is entirely assigned to the individual vehicle mode until $\frac{\delta F_c(K_c)}{\delta K_c} = \frac{\delta F_t(K_t)}{\delta K_t}$. It is also worth noticing that dynamic pricing is required to reach system optimum because $\frac{\delta F_c(K_c)}{\delta K_c}$ changes with K_c. Especially, the pricing is lower when traffic becomes saturated due to the concave shape of $F_c(K_c)$.

4. APPLICATION TO TRANSPORTATION NETWORK SERVICES OPTIMIZATION

The section aims to use the p-MFD as a powerful tool to compare and design optimal control strategies. Firstly, we assume that τ can depend on the passenger demand, i.e. τ is dynamic. According to this assumption, it makes it possible to compare the upper envelope of the associated p-MFD. Secondly, p-MFDs are used to investigate how DBLs

406 impact the transportation system performance and may be a powerful tool to increase
407 capacity even in UE case.

408

409 **4.1. Optimal bus headway**

410

411 When buses and cars share the same network, buses tend to constrain traffic flow
412 because of their lower speed. They may act as moving bottleneck that create local
413 capacity reductions. Intuitively, the occurrence of these reductions increases with the
414 frequency of the bus system (Xie et al., 2013). Consequently, an acceptable trade-off
415 between the bus frequency and the impact on the capacity of the car-MFD must be
416 determined to ensure an efficient performance of the transportation network.

417

418 To cope with this issue, the p-MFD is an adapted tool to calculate the optimal bus time-
419 headway to reach the system optimum. To this end, the car MFD now accounts for the
420 effects of buses. *q(k)* is parameterized by the bus system characteristics. Figure 7a
421 highlights the influence of the bus time-headways on car MFD. As previously mentioned,
422 an increase of h_{bus} reduces the capacity for cars. To mimic this influence, the maximal
423 capacity of cars q_x now depends on the headway:

424 $$q_x(h) = \left(n - e^{1-\frac{h}{h_m}}\right).q_x/n \qquad (13)$$

425 where h_m is the minimal acceptable headway (here h_m=1min). Notice that we can obtain
426 more realistic MFD estimates by extending the work of Boyaci and Geroliminis (2011)
427 and Xie et al. (2013) to the network level. However, this section only aims to introduce
428 the general methodology to determine optimal bus time-headways.

429

430 Car MFDs are now directly related to the value of the bus time-headway *h,* see dotted
431 lines in Figure 7a. These lines correspond to *h* ranged between 1 min and 30 min. Notice
432 that the number of bus in operation n_{bus} changes with *h* but remains independent to the
433 traffic conditions for a given *h*. Moreover, Figure 7a also shows the associated p-MFDs in
434 case of SO situation. This is clearly the most pertinent case to address for a city or transit
435 manager. For a given passenger demand, managers seek to maximize the average speed
436 on the transportation network, i.e. to minimize the average density. The upper envelope
437 *Up* of the calculated p-MFDs corresponds to the set of the optimal situations:

$$U_p(K) = \max_K [P(K)] \qquad (13)$$

It ensures that the average speed is always maximal. Figure 7a highlights in red this upper envelope. Consequently, p-MFD provides the optimal bus time-headway with regard to the passenger demand. Figure 7b depicts the evolution of the optimal bus time-headway with the passenger density. It turns out that very high bus frequencies are required to reach high capacities. Unfortunately, such frequencies are very difficult to maintain in practice. It is also worth noticing that the assumptions made to account for the effects of bus in car MFD formulation strongly impacts the results. However, the methodology proposed here can also be applied for a more realistic car MFD coming from simulation as in (Chiabaut, 2014).

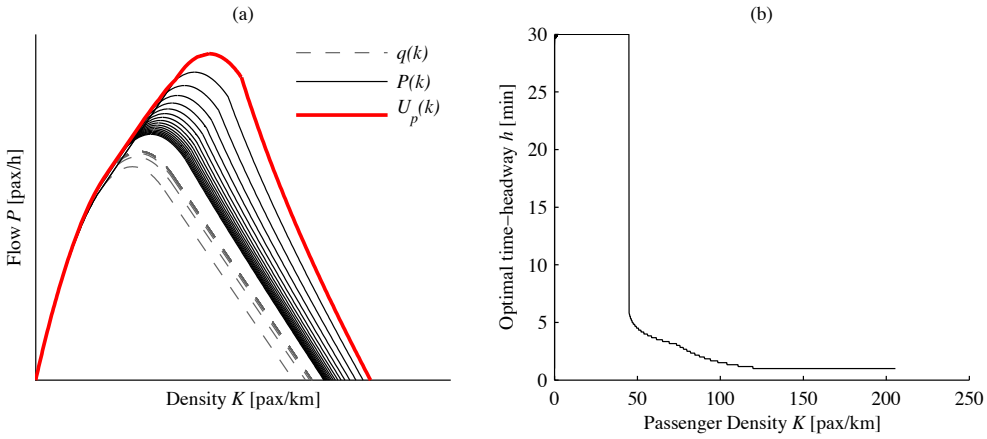

Figure 7: (a) Impact of the bus system on car MFD (b) upper bound of the transportation system

4.2. Comparison of control strategies

After considering only mixed traffic stream, we seek now to incorporate DBL in the formulation of the p-MFD. The final goal is to compare different traffic management strategies to improve the transportation network performance. Consequently, we only consider user equilibrium situations in this section of the paper.

The creation of DBL within the network engenders a capacity reduction for the cars. To make this phenomenon explicit, consider here that α is the ratio of lanes fully dedicated to a rapid public transport mode such as buses or trams. As Gonzales and Daganzo

(2012), we assume that the car MFD is homogenously reduced of α times its original formulation:

$$q_{DBL}(k) = \alpha q(k) \qquad (14)$$

As previously mentioned, the works of (Xie et al., 2013) can be easily adapted to estimate a more accurate MFD. Because these considerations are out of the scope of the paper, the maximal capacity for cars is now equal to $\alpha.q_x$ and the critical speed u_c remains constant for both cases of trapezoidal and curved car MFD.

We can theoretically segregate the public transport system into two parts: (i) a rapid transit system that can use the DBL network and (ii) the remainder of the fleet. Notice that the fleet size is equal for both studied cases. To mimic the effects of DBL on the transit system, we consider that the average speed of vehicles (buses or trams) using the DBL is increased. From a macroscopic lens, they have an average speed $u_t^1 > u_t$. The fleet of the buses that cannot use the DBLs keeps an average speed equal to u_t.

We apply equation (3) to determine the associated p-MFD in the case of UE. Figure 8 presents the results. Notice that the fleet size is assumed constant and the only changing variables are K (and P) and the α ratio that ranges between 0.5 and 1. Figure 8a highlights the main difference between DBL and mixed cases (α is equal to 0.8). It is not surprising to observe that rapid system is competitive before the remainder of the transit system because of their higher average speed. Thus individual car is the only used mode until the speed is reduced to the average speed of rapid system u_t^1. The remaining of the bus fleet becomes advantageous when the situation is enough congested, see the DBL optimal area in Figure 8a. Notice that the switching traffic conditions are directly given by the speed of the different modes. This process can be extended to any number of modes. It is also worth noticing that, even in a very congested situation, the flow of the p-MFD associated to the DBL case is never null. Indeed, we have assumed that the DBLs are never blocked by traffic congestion.

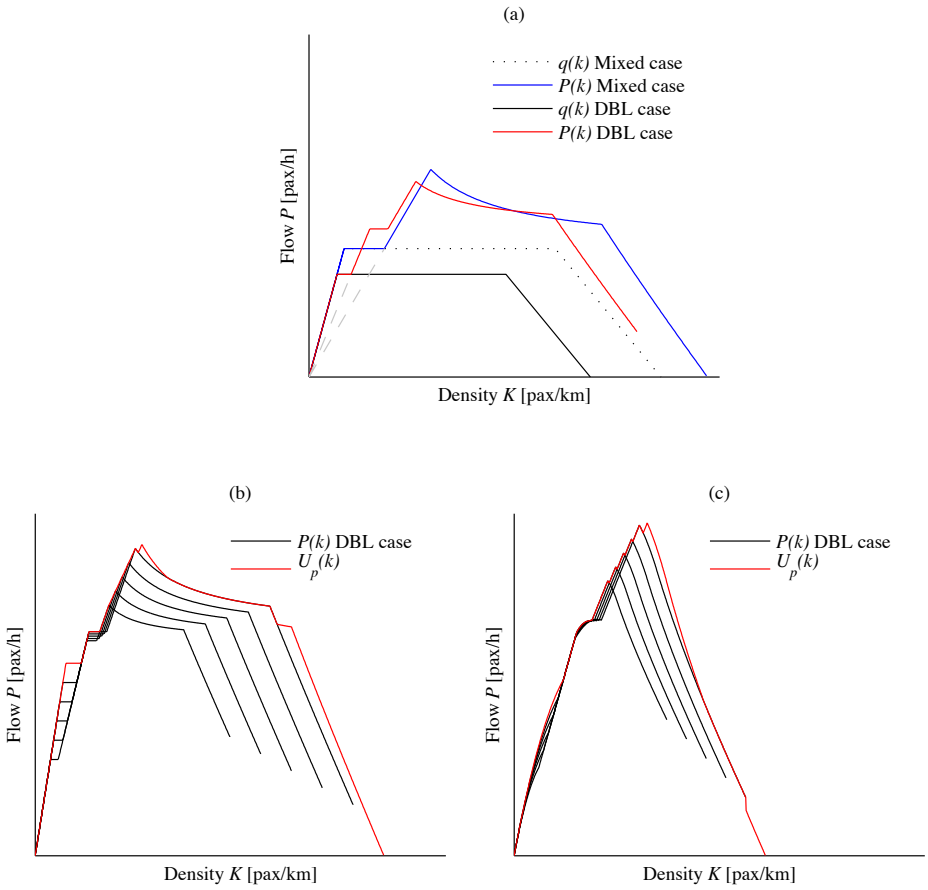

Figure 8: (a) Impact of DBL creation in case of UE and optimal domains of application for (b) a car trapezoidal MFD (c) a parabolic-linear MFD

Finally, we can identify the optimal domains of application in case of UE. As previously mentioned, optimal domains are determined by identifying solutions that maximize the flow for a given density, i.e. maximize the average speed. The red curves depict the upper bound of p-MFD calculated for α-values comprised between 0.5 and 1. In the simplest case of trapezoidal car-MFD, Figure 8b highlights that the creation of DBLs can increase the capacity in free-flow conditions. It is also worth noticing that p-MFD for DBL case never reached a null-flow in congested situations. Indeed, DBL ensures that the bus system can still operate even in very congested states. Similar observations can be formulated in the case of curved-MFD, see Figure 8c. It turns out that DBL can be an optimal strategy in case of UE. This is very promising because global transportation network performance can be increased by promoting public transport even in the case of UE.

5. CONCLUSION

This paper developed tools to analytically assess the performance of a multimodal transportation network. To this end, the paper extends the MFD definition to account for the average number of passengers in each mode. The objective is to obtain a unique function to determine the domains of relevance of different transit strategies, where the system cost is minimized.

First analytical considerations introduce the concept of p-MFD and study its sensitivity to the bus system characteristics in case of a static mode choice. Then, the assumption is relaxed to unveil the impacts of the mode choice on the transportation network performance. Consequently, the user equilibrium case can be compared to the system optimum situation.

This theoretical canvas can then be used to cross compare different transit strategies and to design the optimal bus system characteristics. Especially, the paper focuses on determining the more efficient bus time headway in case of mixed traffic. Then, the study is devoted to the introduction of DBL. The p-MFD permits to determine the optimal domains of application of DBL.

We acknowledge that the approach proposed in the paper is highly conceptual and applied to a very idealized network. However, such an approach makes it possible to provide a general modeling framework that can then be adapted to a large range of situations. Nonetheless, this idealized analysis provides insights into how to assess the global performance of a multimodal transportation network and how to compare different traffic management strategies.

Finally, the results of this paper can be generalized for any design of the network. One of the next extensions is to deal with a spatial distribution of traffic conditions on the network. Indeed, the assumption of uniform distribution of flows can be relaxed allowing for heterogeneous OD demands and mode choice ratio. Moreover, the work can be extended to account for the feedback on the multimodal demand. Indeed, a fixed demand has been considered in the paper but traffic conditions may induce less or more

544 demand that have to be accounted for when calculating the p-MFD. More realistic car
545 MFD formulation can also be considered by resorting to simulation as in (Chiabaut et al.,
546 2014) or more sophisticated estimation method (Hans et al., 2014a). Finally, a last step
547 will be to estimate the p-MFD from field data. This task clearly requires very detailed
548 data (passenger counts, vehicle occupancies, OD matrix, etc.). Urban mobility simulation
549 software may provide synthetic but insightful measurements to estimate more realistic
550 p-MFD.
551

552 **REFERENCES**

553 Aboudolas, K., Geroliminis, N., 2013, Perimeter and boundary flow control in a multi-
554 reservoir heterogeneous networks, *Transportation Research Part B* 55, 265-281.
555 Boyaci, B., Geroliminis, N., 2011, Estimation of the network capacity for multimodal
556 urban systems, *Procedia - Social and Behavioral Sciences* 16, 806-813.
557 Chiabaut, N., 2014, Investigating Impacts of Pickup-Delivery Maneuvers on traffic flow
558 dynamics, *Procedia - Social and Behavioral Sciences*, to be published.
559 Chiabaut, N., Xie, X., Leclercq, L., 2014, Performance analysis for different designs of a
560 multimodal urban arterial, *Transportmetrica B: Transport Dynamics, 2(3), 229-245*.
561 Daganzo, C.F., 2007, Urban gridlock: macroscopic modeling and mitigation approaches.
562 *Transportation Research Part B* 41(1), 49-62.
563 De Jong, D., Knoop, V.L., Hoogendoorn, S.P., 2013, The effect of signal settings on the
564 macroscopic fundamental diagram and its applicability in traffic signal driven
565 perimeter control strategies, *IEEE Conference on Intelligent Transportation Systems,*
566 *Proceedings ITSC,* 1010-1015.
567 Eichler, M., Daganzo, C. F., 2006, Bus lanes with intermittent priority: Strategy formulae
568 and an evaluation, *Transportation Research Part B* 40(9), 731-744.
569 Geroliminis, N., Boyaci, B., 2012, The effect of variability of urban systems characteristics
570 in the network capacity, *Transportation Research Part B* 46, 1607-1623.
571 Geroliminis, N., Daganzo, C.F., 2008, Existence of urban-scale macroscopic fundamental
572 diagrams: some experimental findings, *Transportation Research Part B* 42(9), 759-
573 770.
574 Geroliminis, N., Zheng, N., Aboudolas, K., 2014, Document A three-dimensional
575 macroscopic fundamental diagram for mixed bi-modal urban networks*,*
576 *Transportation Research Part C* 42, 168-181.
577 Godfrey, J., 1969, The mechanism of a road network, *Traffic Engineering and Control*
578 11(7), 323-327.
579 Gonzales, E.J., Daganzo, C.F., 2012, Morning commute with competing modes and
580 distributed demand: user equilibrium, system optimum, and pricing, *Transportation*
581 *Research Part B* 46(10), 1519-1534.
582 Haddad, J., Geroliminis, N., 2012, On the stability of traffic perimeter control in two-
583 region urban cities, *Transportation Research Part B* 46, 1159-1176.

584 Haddad, J., Shraiber, A., 2014, Robust perimeter control design for an urban region,
585 *Transportation Research Part B* 68, 315-332.
586 Hans, E., Chiabaut, N., Leclercq, L., 2014, Investigating the irregularity of bus routes:
587 highlighting how underlying assumptions of bus models impact the regularity
588 results, *Journal of Advanced Transportation*, http://dx.doi.org/10.1002/atr.1275.
589 Hans, E., Chiabaut, N., Leclercq, L., 2014a, A Clustering Approach to Assess the Travel
590 Time Reliability of Arterials, *Transportation Research Record: Journal of the*
591 *Transportation Research Board*, 2422, 42-49.
592 Keyvan-Ekbatani, M., Kouvelas, A., Papamichail, I., Papageorgiou, M., 2012, Exploiting the
593 fundamental diagram of urban networks for feedback-based gating, *Transportation*
594 *Research Part B* 46, 1393-1403.
595 Leclercq, L., Geroliminis, N., 2013, Estimating MFDs in Simple Networks with Route
596 Choice, *Transportation Research Part B* 57, 468-484.
597 Leclercq, L., Chiabaut, N., Trinquier, B., 2014, Macroscopic fundamental diagram: a cross-
598 comparison of estimation method, *Transportation Research Part B* 62, 1-12.
599 Mahmassani, H.S., Williams, J.C., Herman, R., 1984, Investigation of the network-level
600 traffic flow relationships: some simulation results, *Transportation Research Record*
601 971, 121-130.
602 Ramezani, M., Haddad, J., Geroliminis, N., 2015, Dynamics of heterogeneity in urban
603 networks: aggregated traffic modeling and hierarchical control, *Transportation*
604 *Research Part B* 74, 1-19.
605 Wardrop, J.G., 1952, Some theoretical aspects of road traffic research, *Institution of Civil*
606 *Engineers* 2, 325-378.
607 Xie, X., Chiabaut, N., Leclercq, L., 2013, Macroscopic Fundamental Diagram for Urban
608 Streets and Mixed Traffic: Cross-comparison of Estimation Methods. *Transportation*
609 *Research Record* 2390, 1-10.
610 Zheng, N., Geroliminis, N., 2013, On the distribution of urban road space for multimodal
611 congested networks, *Transportation Research Part B* 57, 326-341.